04

The initial stages of the formation of a pulsed discharge in a gap with a tip–plane geometry in preionized argon

© V.S. Kurbanismailov[1], D.V. Tereshonok[2], G.B. Ragimkhanov[1], Z.R. Khalikova[1]

[1] Dagestan State University, Makhachkala, Dagestan Republic, Russia
[2] Joint Institute for High Temperatures, Russian Academy of Sciences, Moscow, Russia
E-mail: gb-r@mail.ru

Received October 28, 2021
Revised December 14, 2021
Accepted December 16, 2021

The study of the effect of the initial conditions on the features of the formation and development of the anodic ionization wave between two electrodes with a tip–plane gap geometry in argon at atmospheric pressure is performed on the basis of a two-dimensional axisymmetric drift–diffusion model.

Keywords: gas discharge, low–temperature plasma, gas breakdown, ionization waves, simulation.

DOI: 10.21883/TPL.2022.03.53525.19067

Regardless of a great number of papers devoted to investigation of pulsed space discharges, a lot of issues connected with the physics of formation of the initial stages stimulate scientific discussions [1–4], including those concerning inert gases [5,6].

In this work, a theoretical/computational investigation of the initial stage of pulsed discharge formation in argon in the inter–electrode gap of the tip–plane geometry was performed for the case of uniform preionization of argon at the atmospheric pressure. The tip (cathode) was shaped as a straight cylinder 1 mm in radius and 1 cm in length, the tip to plane distance was 8.5 mm.

The authors believe that the cathode geometry is just that causes interest to this definition of the problem. In simulation, the cathode is typically represented as a needle with a tapered or rounded tip, which automatically ensures the maximal field strength on the discharge gap axis. In this work, a model of a straight cylinder was used, which creates prerequisites for the toroidal geometry of the ionization wave since the maximal field is concentrated near the cylinder end.

The simulation was performed in the framework of axisymmetric statement of the problem with the initial concentrations of electrons and atomic ions of $10^8\,\mathrm{cm}^{-3}$ over the entire computational space. The electrode voltage was 5 kV during the entire computational period.

A rectangular computational grid clustering towards the discharge axis was used; the grid mesh number was $N_r = 1050$. In the inter–electrode gap, the grid clustered near the electrodes ($N_z = 1900$).

The gas–discharge plasma is regarded as a continuous multicomponent medium consisting of neutral atoms (ar), electrons (e), excited atoms (Ar^*) with the excitation energy of 11.5 eV, atomic (Ar^+) and molecular (Ar_2^+) ions. The kinetics of the processes under consideration and constants of relevant reactions (except for direct ionization and excitation) were taken from [7].

The equation set presented below comprises balance equations for charged and excited particles, electron energy equation and Poisson equation [7–10]. Heating of the neutral gas was ignored. In calculation, the heavy particles temperature was assumed to be equal to that of the neutral gas (300 K).

$$\frac{\partial n}{\partial t} + \nabla \cdot \mathbf{\Gamma} = S,$$

$$\mathbf{\Gamma} = q n \mu \mathbf{E} - D \nabla n,$$

$$\frac{\partial}{\partial t}\left(\frac{3}{2} n_e k_\mathrm{B} T_e\right) + \nabla \cdot \mathbf{F} = \mathbf{j}_e \cdot \mathbf{E} + S_e,$$

$$\mathbf{F} = \frac{5}{2} k_\mathrm{B} T_e \mathbf{\Gamma}_e - \lambda_e \nabla T_e,$$

$$\lambda_e = \frac{5}{2} n_e D_e,$$

$$\nabla \cdot \mathbf{E} = \frac{e(n_{\mathrm{Ar}^+} + n_{\mathrm{Ar}_2^+} - n_e)}{\varepsilon_0}, \qquad (1)$$

where n, $\mathbf{\Gamma}$, μ, D are the concentration, flowrate, mobility and diffusion coefficient of the respective plasma components, e is the electron charge, k_B is the Boltzmann constant, T_e is the electron temperature, λ_e, D_e is the heat conductance and diffusion coefficient governed by the reduced local field E/N from BOLSIG+ [11], n_e, n_{Ar^+}, $n_{\mathrm{Ar}_2^+}$ are the concentrations of electrons, atomic ions and molecular ions, S is the source of generation and annihilation of the considered plasma particles, S_e are the elastic and inelastic electron losses, $\mathbf{j}_e$ is the electron current density, $\mathbf{E}$ is the electric field strength. We have $q = +1$ for ions, $q = -1$ for electrons, $q = 0$ for excited particles.

The excitation and direct–ionization constants were governed by reduced local field E/N from BOLSIG+ [11]. Other constants were defined as functions of T_e.

The ion mobility coefficients and diffusion coefficient of excited eigen-gas particles were taken from [12].

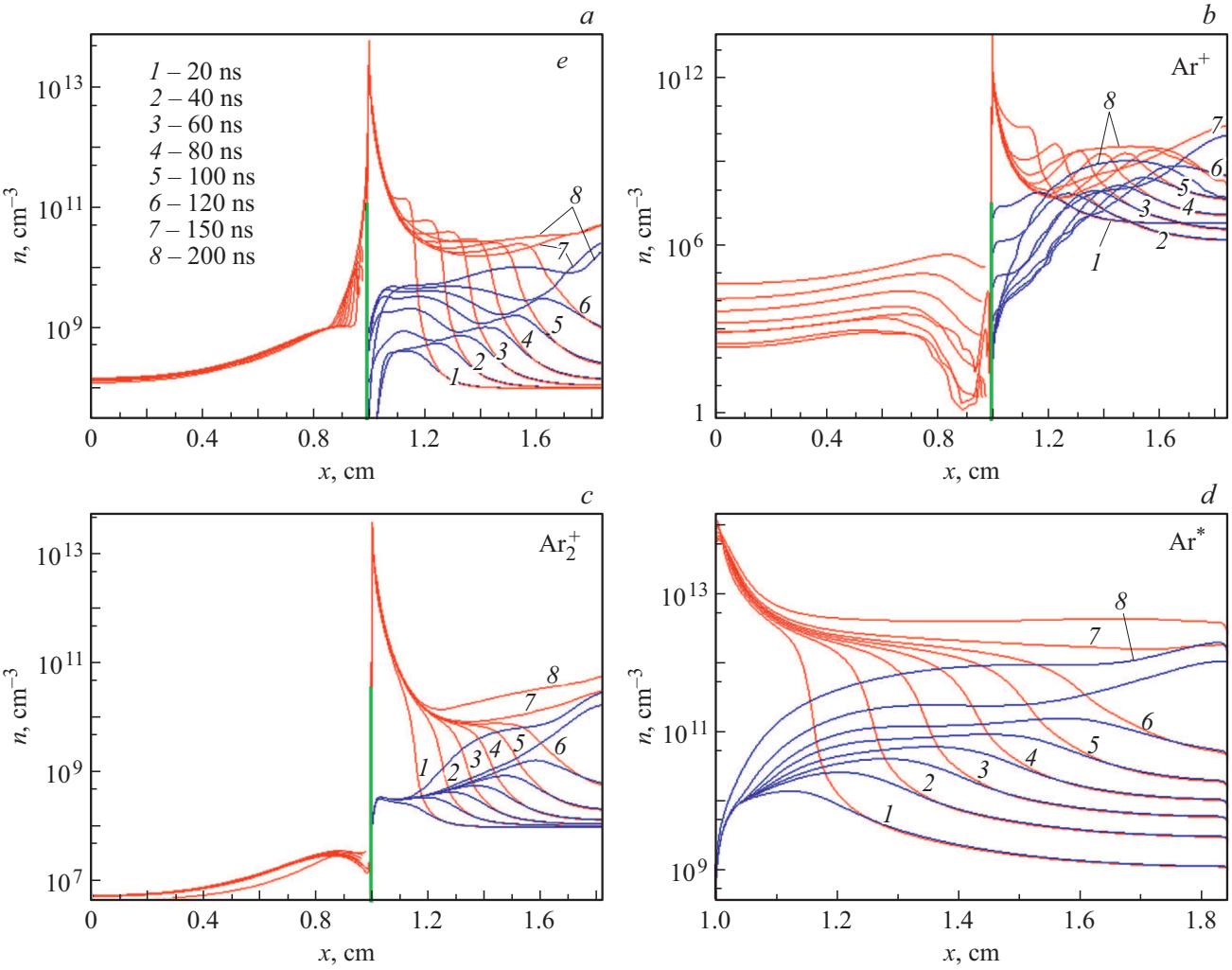

Figure 1. Concentration distributions of electrons (a), atomic argon ions Ar^+ (b), molecular argon ions Ar_2^+ (c), and excited argon ions Ar^* (d) within the discharge gap for different time moments. Blue lines are for $r = 0$, red lines are for $r = 0.1$ cm. The colored figure is given in the electronic version of the paper.

Boundary conditions for the potential, charged particles and excited particles n^* (sub-index i designates atomic and molecular ions) at the cathode were

$$\varphi_c = 0, \quad \frac{\partial n_i}{\partial z} = 0, \quad \mathbf{\Gamma}_e = -\gamma \sum_i \mathbf{\Gamma}_i,$$

$$n^* = 0, \quad \frac{3}{2} k_B T_e = I - 2\varphi_W,$$

at the anode

$$\varphi_a = V_a, \quad \frac{\partial n_e}{\partial z} = 0, \quad \frac{\partial T_e}{\partial z} = 0, \quad n_i = 0, \quad n^* = 0,$$

at the computational space side edges

$$\frac{\partial \varphi}{\partial r} = 0, \quad \frac{\partial n_e}{\partial r} = 0, \quad \frac{\partial n_i}{\partial r} = 0, \quad \frac{\partial n^*}{\partial r} = 0, \quad \frac{\partial T_e}{\partial r} = 0,$$

where $\gamma = 0.1$ is the second Townsend coefficient, $I = 15.76$ eV is the argon ionization potential, $\varphi_W = 4.5$ eV is the cathode work function, V_a is the anode potential. For the ion–electron emission, the cathode–directed flows of both atomic and molecular ions were considered.

The convection–diffusion equations were solved by the finite volume method [13]. The Poisson equation was solved by the iterative alternating-direction method.

Fig. 1 presents characteristic distributions of concentrations of electrons (a), atomic argon ions Ar^+ (b), molecular argon ions Ar_2^+ (c), and excited argon ions Ar^* (d) in the gap for different time moments at $r = 0$ and 0.1 cm.

The analysis of calculations shows (Fig. 1, a–d) that at the initial stage of charge formation an anode–directed ionization wave arises in the discharge gap. Notice that the concentrations of charged and excited particles in the gap have maxima near the tip edge at 0.1 cm from the discharge axis; this is caused by edge effects, since the tip has a cylindrical shape and, hence, the tip–edge field is higher

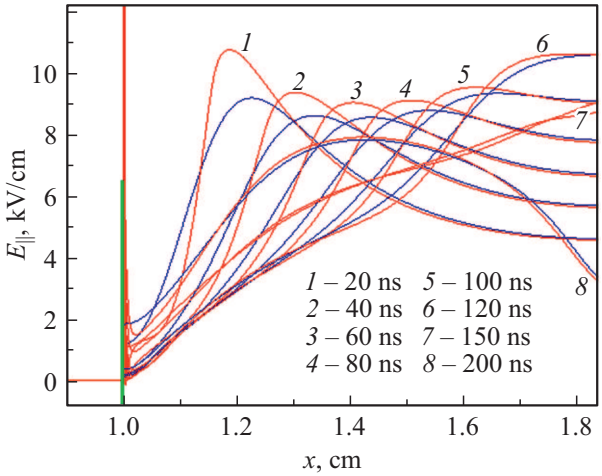

Figure 2. Amplitude distribution of the electric field E longitudinal component in the discharge gap at different time moments. Blue lines are for $r = 0$, red lines are for $r = 0.1$ cm. The colored figure is given in the electronic version of the paper.

(Fig. 2) than that at the axis, which leads to a more intense ionization.

In the course of time, the concentration of atomic argon ions Ar^+ (Fig. 1, *b*) at the axis ($r = 0$ cm) in the gap increases, and its maximum shifts towards the anode. By the time moment of 150 ns, the concentration is maximal near the anode, while by 200 ns the ion concentration is maximal in the center of the tip–anode gap. The same pattern is observed for the concentration of molecular ions Ar_2^+ (Fig. 1, *c*), but the Ar_2^+ concentration in the gap is higher than that of Ar^+ and of excited argon ions Ar^* (Fig. 1, *d*), which indicates high intensity of the processes of molecular ions formation in the gap during the conversion. When gas pressures are high and temperature is low (at the initial stage of formation, gas has no enough time to get heated), development of molecular ions takes place.

As the obtained results show, when voltage $V_a = 5$ kV is applied to the gap, the velocity of an anode–directed wave remains constant (close to $5 \cdot 10^6$ cm/s) in the time interval of 20 to 120 ns (Fig. 2) regardless of strong nonuniformity of electric field E (Fig. 2) due to the specific geometry of the discharge gap. At the moment of the wave arrival to the anode, the electron concentration at the discharge axis is maximal near the anode, however, the electron concentration at the tip edge (0.1 cm from the center) remains the highest one over the entire gap, which may be explained by that field E (Fig. 2) is higher than that at the discharge axis.

Notice the qualitative agreement with other calculations of the electric field E behavior along the discharge axis for argon in the tip–plane geometry [5], where E first drops and then increases with approaching the anode.

In this work, 2D simulation was performed of the pulsed discharge formation in the atmospheric–pressure argon in the gap with the tip–plane geometry.

It was shown that, at the stage of formation, reaction $Ar + Ar + Ar^+ \rightarrow Ar + Ar_2^+$ results in that the concentration of molecular argon ions Ar_2^+ significantly exceeds the concentration of atomic ions Ar^+, which is caused by slight destruction of Ar_2^+ due to the absence of gas heating. It was established that an anode–directed ionization wave is formed in the discharge gap at time moments earlier than 200 ns. Despite the strong nonuniformity of the electric field, the velocity of the anode–directed wave remains constant and equal to $5 \cdot 10^6$ cm/s.

Financial support

The study was supported by the Russian Fundamental Research Foundation (grant № 19-08-00333a).

Conflict of interests

The authors declare that they have no conflict of interests.

References

[1] Yu.D. Korolev, G.A. Mesyats, *Fizika impul'snogo proboya gazov* (Nauka, M., 1991) (in Russian).
[2] V.F. Tarasenko, E. Baksht, A.G. Burachenko, M.I. Lomaev, D.A. Sorokin, Yu.V. Shut'ko, Tech. Phys. Lett., **36** (4), 375 (2010). DOI: 10.1134/S1063785010040255.
[3] G.V. Naidis, V.F. Tarasenko, N.Yu. Babaeva, M.I. Lomaev, Plasma Sources Sci. Technol., **27** (1), 013001 (2018). DOI: 10.1088/1361-6595/aaa072
[4] V.V. Osipov, Phys. Usp., **43** (3), 221 (2000). DOI: 10.1070/pu2000v043n03ABEH000602.
[5] Y. Sato, K. Ishikawa, T. Tsutsumi, A. Ui, M. Akita, S. Oka, M. Hori, J. Phys. D: Appl. Phys., **53** (26), 265204 (2020). DOI: 10.1088/1361-6463/ab7df0
[6] A. Sobota, F. Manders, E.M. van Veldhuizen, Jan van Dijk, M. Haverlag, IEEE Trans. Plasma Sci., **38** (9), 2289 (2010). DOI: 10.1109/TPS.2010.2056934
[7] M. Baeva, A. Bösel, J. Ehlbeck, D. Loffhagen, Phys. Rev. E, **85** (5), 056404 (2012). DOI: 10.1103/PhysRevE.85.056404
[8] D.V. Tereshonok, Tech. Phys. Lett., **40** (2), 135 (2014). DOI: 10.1134/S106378501402014X.
[9] S.T. Surzhikov, *Fizicheskaya mekhanika gazovykh razryadov* (Izd-vo MGTU im. N.E. Baumana, M., 2006) (in Russian).
[10] V.S. Kurbanismailov, O.A. Omarov, G.B. Ragimkhanov, D.V. Tereshonok, Tech. Phys. Lett., **43** (9), 853 (2017). DOI: 10.1134/S1063785017090206.
[11] G.J.M. Hagelaar, L.C. Pitchford, Plasma Sources Sci. Technol., **14** (4), 722 (2005). DOI: 10.1088/0963-0252/14/4/011
[12] B.M. Smirnov, *Svoystva gazorazryadnoy plazmy* (Izd-vo Politekhn. un-ta, SPb, 2010) (in Russian).
[13] J. Teunissen, Plasma Sources Sci. Technol., **29** (1), 015010 (2020). DOI: 10.1088/1361-6595/ab6757